Modeling Helioseismic Signatures of Meridional Circulation

Andrey M. Stejko[1], Alexander G. Kosovichev[1,] Valery V. Pipin[2]

[1]NJIT, [2]Institute of Solar-Terrestrial Physics, Irkutsk, Russia

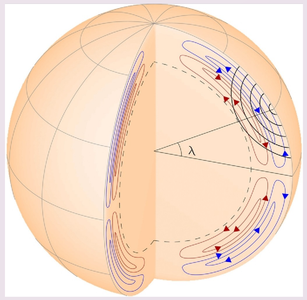

Figure 1. from Detection of Equatorward Meridional Flow and Evidence of Double-cell Meridional Circulation inside the Sun; Zhao et al. 2013 ApJL 774 L29 doi:10.1088/2041-8205/774/2/L29

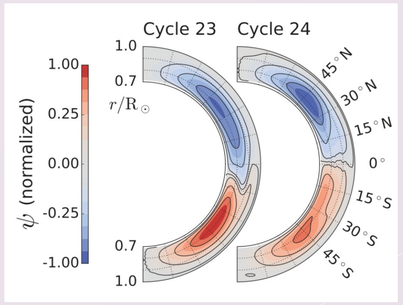

Figure 2. from Meridional flow in the Sun's convection zone is a single cell in each hemisphere; Gizon et al. 2020 Science 368 1469 doi:10.1126/science.aaz7119

Introduction

In this poster we present a new 3D numerical solver of the linearized compressible Euler equations (GALE). Acoustic oscillations are computed over 3D background velocity fields which can be used to test the effects of theoretical models of internal solar velocities. With inferences of a double-cell meridional circulation (Zhao et al. 2013, Figure 1) made using HMI observations, along with recent reassertions of a single-cell model (Gizon et al. 2020, Figure 2) from MDI/GONG data, it becomes obvious that in-depth investigation of the limit of helioseismic techniques is required. To that end we use a "forward-modeling" approach to test four different profiles (M1, M2, K1, and K2) of meridional circulation, generated by the mean-field models of Pipin & Kosovichev (2018, 2019). M1 and M2 are models of single-cell and double-cell meridional circulation, created with minimal physics based parameter changes that let us estimate the low-end baseline for whether differences between the two regimes can be spotted within the error of travel-time difference measurements. Models K1 and K2 are physics based models that are more consistent with results of Zhao et al. (2013) and Gizon et al. (2020) respectively.

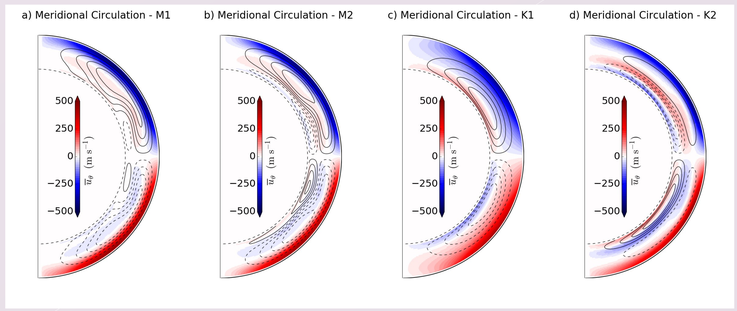

Figure 3. Latitudinal velocities, generated by the mean-field models of Pipin & Kosovichev (2019) (M1 and M2) and Pipin & Kosovichev (2018) (K1 and K2 – referred to as M2 and M3 in their paper). Meridional circulation models are amplified by a factor of 36.

Model Description

The GALE (Global Acoustic Linearized Euler) algorithm (Stejko et al. 2021) solves the conservation form of the linearized compressible Euler equations on a fully global 3-dimensional grid: $0 \le \varphi \le 2\pi$, $0 < \theta < \pi$, $0 < r \le R$. The linear approximation is solved for perturbations of the potential flow field (denoted by a prime), over background field terms (denoted by a tilde) derived from the standard solar model S (Christensen-Dalsgaard et al. 1996).

$$\frac{\partial \rho'}{\partial t} + \mathrm{Y}' = 0$$

$$\frac{\partial \mathrm{Y}'}{\partial t} + \nabla : \left(\rho' \tilde{\boldsymbol{u}} \tilde{\boldsymbol{u}} + \tilde{\rho} \boldsymbol{u}' \tilde{\boldsymbol{u}} + \tilde{\rho} \tilde{\boldsymbol{u}} \boldsymbol{u}'\right) = -\nabla^2 (p') - \nabla \cdot (\rho' \tilde{g}) + \nabla \cdot S$$

$$\frac{\partial p'}{\partial t} = -\frac{\Gamma_1 \tilde{p}}{\tilde{\rho}} \left[\nabla \cdot \tilde{\rho} \boldsymbol{u}' + \rho' \nabla \cdot \tilde{\boldsymbol{u}} - \frac{p'}{\tilde{p}} \tilde{\boldsymbol{u}} \cdot \nabla \tilde{\rho} + \tilde{\rho} \boldsymbol{u}' \cdot \frac{N^2}{g} \right]$$

Y is defined as the divergence of the momentum field $\boldsymbol{m}$ ($\mathrm{Y} = \nabla \cdot \boldsymbol{m} = \nabla \cdot \rho \boldsymbol{u}$), computing perturbations in the potential flow field and omitting solenoidal terms in our governing equations. Perturbations are initiated by a randomized source function (S), mimicking the stochastic excitation of acoustic modes in the convective interior.

Figure 4. The N-S travel-time differences ($\delta\tau_{NS}$) as a function of travel distance (Δ) for models M1 (a), M2 (b), K1 (c) and K2 (d). The travel-time measurements are shown under the application of a Gaussian phase-speed filter ($\sigma = 0.05 v_p$) for 5 latitudinal averages spanning 30°N−50°N, 10°N−30°N, 10°S−10°N, 10°S−30°S, 30°S−50°S. Dashed lines are theoretical times computed using the ray-path approximation. Error bars show the standard deviation of the measured realization noise. Meridional circulation models are amplified by a factor of 36.

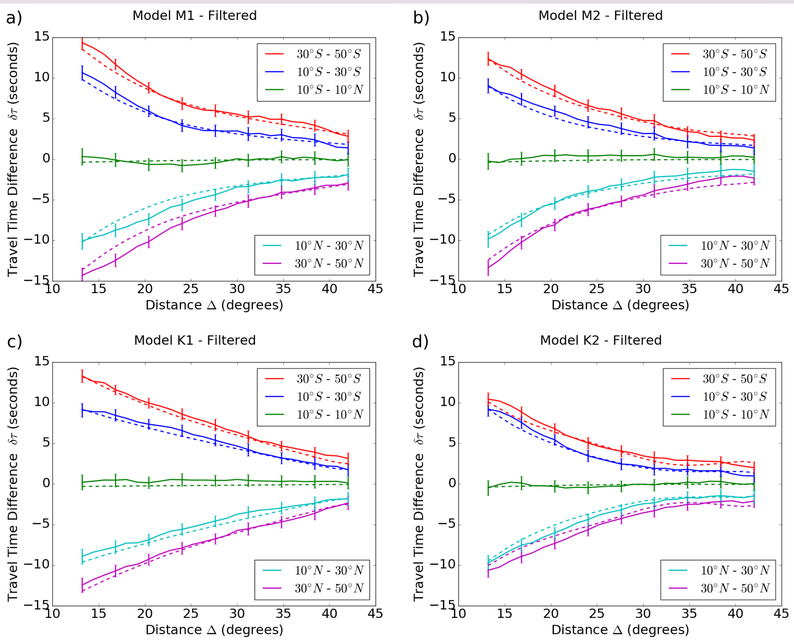

Results

We use the deep focusing method (Zhao et al. 2009), under the application of a phase velocity filter, to measure travel-time differences throughout the convective interior of our model, plotting the great circle travel distances of acoustic rays in Figure 4. In order to simulate the SNR we expect from a decade of solar observations (the operational time-frame of HMI) the strength of the velocity field is amplified by a factor of 36. We compare our travel time differences against values computed using the ray-path approximation (Giles 1999), and see a good agreement with expected results. Error bars show one standard deviation of error in the realization noise measured in our model. This places a bound on theoretically measurable differences in profiles.

A comparison of the 10°S-30°S latitudinal averages with MDI/GONG travel-time differences computed by Gizon et al. (2020) shows that it should be possible to theoretically distinguish large profile differences such as K1 ad K2, however, since models M1 and M2 fall within one standard deviation of realization noise, it is difficult to say with any degree of certainty that meridional circulation is either single- or double-cell.

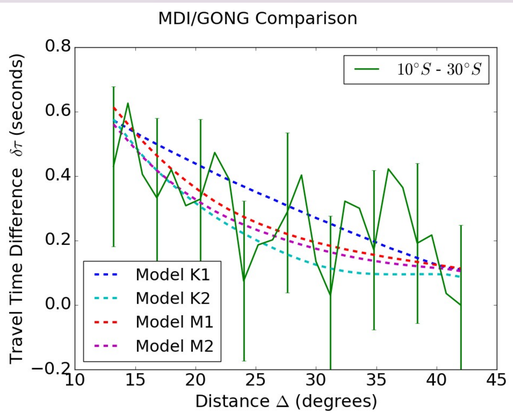

Figure 5. The N-S travel-time differences ($\delta\tau_{NS}$) as a function of travel distance (Δ) for MDI/GONG data published by Gizon et al. (2020). Latitude ranges in both hemispheres (10°N−30°N, 10°S−30°S) are averaged in order to reduce noise and are compared to dashed lines representing latitudinal averages for models K1, K2, M1, and M2 as measured using the ray-path approximation .

Conclusion

High levels of noise in measurements leave large uncertainties that may be the source of some of the divergent conclusions made on the nature of meridional circulation. Physics-based models can be used to constrain results in the context of a broader complex systems. We analyze differences between a shallow single-cell and a weak-reversal double-cell regime, generated by a mean-field simulation that uses a physics-based model of gyroscopic pumping to induce the reverse-flow cell near the base of the tachocline. In these models, we see that the travel-time differences may fall well within one standard deviation of error for phase-speed filtered deep-focusing measurements. These models (M1 & M2) provide the low-end of the baseline for variance between the two regimes. We also Examine physics-based profiles that may be more consistent with single-cell (Gizon et al. 2020) inferences such as K1 or double-cell (Zhao et al. 2013) inferences such as K2. The deep single-cell profile (K1) and strong-reversal double-cell profile (K2) show large enough differences that a distinction with a relatively high degree of confidence is feasible. For now, however, the best way to constrain these solutions is by looking at the broader impacts of these profiles within the context of their effects on global solar dynamics (see Kitchatinov 2013). In Pipin & Kosovichev (2018) we see that an unavoidable effect of increasing the strength of the return flow is a profile of differential rotation that is inconsistent with inferences of global helioseismology. Mean-field modeling only scratches the surface of the complex dynamics in the solar interior, and the development of mean-field theory in conjunction with forward-modeling of helioseismic signals can be a powerful tool to help interpret helioseismology inversions

Bibliography

- Christensen-Dalsgaard, J., et al. 1996, Science, 272, 1286
- Gizon, L., Cameron, R. H., Pourabdian, M., et al. 2020, Science, 368, 1469
- Kitchatinov, L. L. 2013, in Solar and Astrophysical Dynamos and Magnetic Activity, Vol. 294, 399–410
- Pipin, V. V., & Kosovichev, A. G. 2018, ApJ, 854, 67
- Pipin, V. V., & Kosovichev, A. G. 2019, ApJ, 887, 215
- Stejko, A. M., Kosovichev, A. G., & Mansour, N. N. 2020, ApJS, 253, 9
- Zhao, J., Bogart, R. S., Kosovichev, A. G., Duvall, T. L., J., & Hartlep, T. 2013, ApJ, 774, L29